

Preliminary Cross-Sectional Structural MRI Analysis of Data from the Alzheimer's Disease Neuroimaging Initiative

C. Fennema-Notestine^{1,2}, A. S. Fleisher³, D. J. Hagler, Jr.⁴, E. H. Wu⁵, D. S. Karow⁵, E. T. Han⁶, and A. M. Dale⁷

¹Psychiatry, University of California, San Diego, La Jolla, CA, United States, ²Research Service, VASDHS, San Diego, CA, United States, ³Neurosciences, University of California, San Diego, La Jolla, CA, United States, ⁴Cognitive Science, University of California, San Diego, La Jolla, CA, United States, ⁵Radiology, University of California, San Diego, La Jolla, CA, United States, ⁶Global Applied Science Laboratory, GE Healthcare, Menlo Park, CA, United States, ⁷Neurosciences and Radiology, University of California, San Diego, La Jolla, CA, United States

INTRODUCTION: A non-invasive, *in vivo* MRI biomarker for Alzheimer's disease (AD) would enable earlier clinical diagnosis and aid in monitoring therapeutic effectiveness. Studies in early AD and in individuals with Mild Cognitive Impairment (MCI), many of whom will develop AD, have shown hippocampal and entorhinal cortex to be smaller than in controls and predictive of future conversion to AD. In addition, the cingulate cortex has been shown to exhibit changes in similar cohorts. Ongoing development within the NIH/NICRR sponsored Morphometry Biomedical Informatics Research Network (mBIRN) and the Alzheimer's Disease Neuroimaging Initiative (ADNI) have resulted in procedures for image acquisition, correction, and analysis that enable large, multi-site clinical research studies using brain imaging. Here we present preliminary results from applying these methods to a subset of the initial ADNI cohort, including elderly controls (NC) and individuals with MCI or early AD.

METHODS: ADNI data for 114 controls (mean age 75.7y; mean MMSE 29.0), 115 MCI (74.8y; 27.1 MMSE), and 58 AD (75.9y; 23.4 MMSE) were studied. Dual 3D T1-weighted volumes were downloaded, reviewed for quality, corrected for gradient nonlinearity and B1 field inhomogeneity, registered, and averaged to improve signal-to-noise. Using cerebral segmentation and cortical surface reconstruction methods based on FreeSurfer, regional measures and reconstructed cortical surface volumes were produced and reviewed for technical adequacy. Cerebral segmentation provided regional volumes for hippocampus, amygdala, basal ganglia, thalamus, neocortex, and white matter (Fig 1). Cortical thickness measures also were available for 38 NC (mean age 75.7y; mean MMSE 29.0), 42 MCI (74.5y; 27.3 MMSE), and 35 AD (76.4y; 23.7 MMSE). The cortical reconstruction method created a surface tessellation which was then divided into distinct cortical regions (Fig 2). Results provide continuous high-resolution maps of cortical thickness (Fig 3) and average thickness values for regions of interest. Measures of interest include hippocampus, entorhinal cortex, parahippocampal cortex, posterior cingulate, and lateral ventricular. Regional regression analyses examined group differences while controlling for age.

RESULTS: Region of interest findings confirm previous work in AD, including smaller hippocampal, cortical, and white matter volumes, and thinner entorhinal, parahippocampal, and posterior cingulate cortices, with increased ventricular volumes compared to NC ($p < .05$). MCI individuals were more similar to AD than NC for hippocampus (Fig 3b; AD $p > .05$; NC $p < .001$) and posterior cingulate (Fig 3c; AD $p > .05$; NC $p < .005$). MCI fell between NC and AD for the temporal horn of the lateral ventricle (Fig 3a; AD $p < .001$; NC $p < .005$) and left entorhinal cortex (Fig 3d; AD $p < .05$; NC $p = .06$), and were not different from NC on parahippocampal thickness (Fig 3e; $p > .05$). Comparisons of continuous maps of cortical thickness provide additional localization of group differences and further emphasize a pattern of progression from NC to MCI to early AD. Cortical thickness of NC and AD groups differed by more than 0.5mm in mesial temporal regions and more than .3mm in posterior cingulate and temporo-parietal association areas (Fig 4).

DISCUSSION and CONCLUSIONS: Findings demonstrate the feasibility of mBIRN and ADNI supported large-scale acquisition and image analysis procedures for detecting subtle structural group differences. For the investigation of prodromal AD, these methods provide a wide range of measures within the same subjects. Significant differences were found between NC and MCI within the mesial temporal and posterior cingulate regions, suggesting that some of these measures may be more sensitive to early AD-related changes. Future longitudinal evaluation may provide standardized predictive imaging biomarkers for AD. The ADNI is following these same individuals over time and providing additional data measuring metabolism, neuropsychological performance, CSF markers, and genetics. When combined with high-throughput methods such as those described here, this will enable a more complete characterization of functional and anatomical changes associated with disease progression.

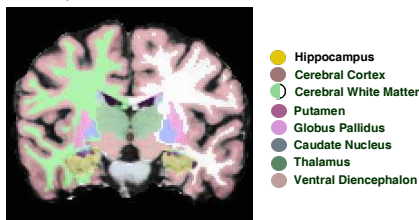


Fig 1. Coronal section cerebral segmentation.

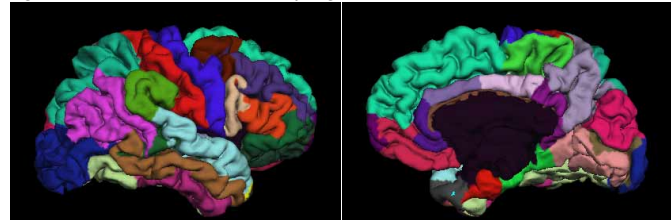


Fig 2. Regions of interest for cortical surface parcellation.

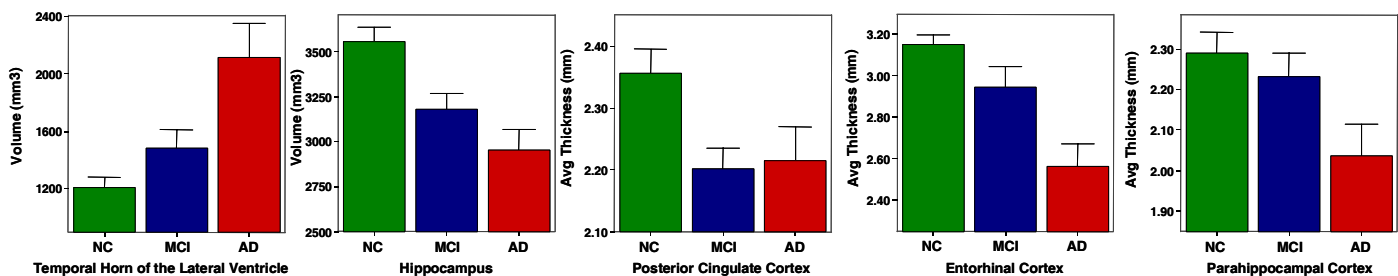


Figure 3. Mean volumetric (mm³) or thickness (mm) by group for left hemisphere Cortex regions of interest a-e; error bars = std error of the mean.

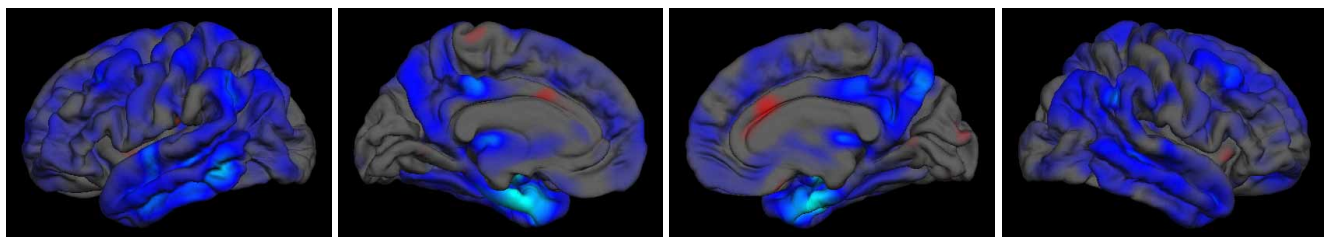


Figure 4. Cortical surface map of average difference in thickness between AD and NC; bright blue represents regions of greatest thickness difference. Scale reflects thickness in mm ranging from -.5 (bright blue) to +.5mm thickness.